Morphology and Mechanical Properties of Binary Blends of Polypropylene with Statistical and Block Ethylene-Octene Copolymers

Guoming Liu,[1,2] Xiuqin Zhang,[1] Chenyang Liu,[1] Hongyu Chen,[3] Kim Walton,[4] Dujin Wang[1]

[1]*Beijing National Laboratory for Molecular Sciences, CAS Key Laboratory of Engineering Plastics, Institute of Chemistry, Chinese Academy of Sciences, Beijing, 100190, China*
[2]*Graduate University of Chinese Academy of Sciences, Beijing, 100190, China*
[3]*The Dow Chemical Company Limited, Shanghai, 201203, China*
[4]*The Dow Chemical Company, Freeport, Texas, 77541*

Received 2 March 2010; accepted 7 July 2010
DOI 10.1002/app.33035
Published online 30 August 2010 in Wiley Online Library (wileyonlinelibrary.com).

ABSTRACT: In the present work, statistical (EOCs) and block (OBCs) ethylene-octene copolymers, with similar densities and crystallinities, were used as impact modifiers of isotactic polypropylene (iPP), and the toughening effects of these two types of elastomers were compared. The viscosity curves of EOCs were similar to those of OBCs with equivalent melt flow rate (MFR), enabling a comparison of the viscosity ratio and elastomer type as independent variables. No distinct differences on the crystal forms and crystal perfection of iPP matrix in various blends were observed by thermal analysis. Morphological examination showed that OBCs form smaller dispersed domains than EOCs with similar MFRs. The flexural modulus, yield stress, stress and strain at break showed the same variation tendency for all the investigated polypropylene/elastomer blends. However, the room temperature Izod impact toughness of iPP/OBC blend was higher than that of iPP/EOC blend containing elastomer with the similar MFRs. The experimental results indicated that the compatibility of iPP/OBCs was much higher than that of iPP/EOCs. © 2010 Wiley Periodicals, Inc. J Appl Polym Sci 119: 3591–3597, 2011

Key words: polypropylene/elastomer blends; olefin block copolymers; ethylene-octene copolymers; mechanical properties

INTRODUCTION

Isotactic polypropylene (iPP) is one of the most widely used polymers because of its low cost, processing ease, and chemical and electrical resistance, however, its low temperature impact toughness is relatively poor, which limits the practical application as a stand-alone polymer. Therefore, many efforts have been made to improve the toughness of iPP, such as toughening with a certain amount of rubber.[1–4] Recently, it was found that rigid organic/inorganic particles can also increase the impact strength of iPP under certain conditions.[5,6] Although rubber toughened iPP has the shortcoming of decreasing overall stiffness, the toughing effect for iPP/rubber blends is much better than that of iPP/rigid particle blends. In the early 1990's, the statistically random copolymers of ethylene and α-olefin became available in industrial quantities based on the INSITE™ constrained geometry catalyst technology of the Dow Chemical Company, which enabled the control of molecular weight, molecular weight distribution and comonomer content in copolymers.[7,8] Polyolefin elastomers, prepared using this technique, have been abundantly used in industry as impact modifiers for iPP. However, due to the statistically random distribution of comonomer sites in the macromolecular chain, the melting temperature (T_m) of this kind of copolymer decreases sharply with increasing comonomer content,[9] thus limiting the applications at high temperature.

In 2006, the Dow Chemical Company developed a chain shuttling catalyst technology, which can produce olefin block copolymers (OBCs) in a continuous process.[10] The block copolymers synthesized by chain shuttling technology are characteristic of high crystalline ethylene-octene hard blocks and low crystalline or amorphous ethylene-octene soft blocks. The high crystalline blocks have very low comonomer content and high melting temperature, and the low crystalline or amorphous blocks have high comonomer content and low glass transition temperature. These new block copolymers have a statistical multiblock architecture with a distribution in block

Correspondence to: D. Wang (djwang@iccas.ac.cn).
Contract grant sponsor: The Dow Chemical Company.
Contract grant sponsor: The China National Funds for Distinguished Young Scientists; contract grant number: 50925313.

TABLE I
Characteristics of Isotactic Polypropylene and Ethylene-Octene Statistical/Block Copolymers

Sample	Density (g/cm^3)	MFR[a] (g/10 min)	M_w (kg/mol)	M_w/M_n	Net octene content[b] (mol%)	Octene content in hard segment[b] (mol%)	Octene content in soft segment[b] (mol%)	Hard segment content (wt %)	Xc, $_{\Delta H}$[c] (wt %)
iPP	0.900	35	–	–	–	–	–	–	–
OBC-1	0.870	0.52	177	2.31	19.7	1.44	27.4	20	10.8
OBC-2	0.868	4.46	109	2.39	20	1.46	27.7	19	12.2
EOC-1	0.863	0.5	182	1.93	14.3	–	–	–	13.5
EOC-2	0.863	5.0	107	1.97	14.5	–	–	–	13.8

[a] Melt flow rate, 2.16 kg, 230°C for iPP, 2.16 kg, 190°C for elastomers.
[b] Determined from ^{13}C-NMR.
[c] Measured by enthalpy of fusion.

lengths and the number of blocks per chain. Compared to statistical ethylene-octene copolymers, the block architecture imparts a substantially higher melting temperature and a higher crystallization temperature, while maintaining a lower glass transition temperature and a better organized crystalline morphology. The hard blocks crystallize as space filling spherulites even as the fraction of crystallizable hard blocks is very low.[11]

The soft segment of OBCs is expected to be compatible with iPP, whereas the hard segments with similar chain architecture to linear low density polyethylene are incompatible with iPP.[12–15] Therefore, it is of interest to determine whether block ethylene-octene copolymers can be designed as iPP impact modifiers and if there are any impact performance differences between block and statistical copolymers for modifying iPP. In this research, two ethylene-octene statistical copolymers and two block copolymers with similar densities and crystallinities were selected to blend with iPP. The morphologies, mechanical properties of the two kinds of blends as well as melting behaviors were investigated.

EXPERIMENTAL

Materials and sample preparation

The iPP with a melt flow rate (MFR) of 35 g/10 min at 230°C/2.16 kg was provided by the Dow Chemical Company (Shanghai, China). Two block ethylene-octene (coded as OBC-1 and OBC-2) copolymers with nearly the same chain composition, but of different molecular weight, were supplied by the Dow Chemical Company (Shanghai, China). Two ethylene-octene statistical copolymers (coded as EOC-1 and EOC-2), with the similar density and crystallinity to the block copolymers, were also supplied by the Dow Chemical Company (Shanghai, China). The basic parameters are given in Table I.

The iPP/elastomer blends (70/30, wt %) were prepared using a corotating twin screw extruder (ZSK-25, D = 25mm and L/D = 48) operated at 200°C and a screw rotation speed of 500 rpm. The output of the extruder was about 22.7 kg/hour. An antioxidant (Irganox B225) was added to the blends with a weight fraction of 0.2% to avoid degradation during processing. The resulting pellets were injection molded using an injection molding machine (Yizhimi UN120A, clamping force 120 ton). A general purpose screw was used in the barrel, with temperatures set at 180, 200, and 210°C from the hopper to the nozzle. The injection point was at the longitudinal axis side of the specimens. Three types of specimens were made: dog-bone tensile bars with width of 3.2 mm, and thickness of 3.2 mm (ASTM D638 Type V); flexural test bars with dimensions of 54.5 × 6 × 4 mm (length × width × thickness); Izod impact test bars with length of 63.5 mm, width of 12.7 mm (10.16 mm under the notch), and thickness of 4 mm. The "V" shaped notch of the impact specimen was cut by a notching cutter after injection molding.

DSC measurements

The melting behaviors of the iPP/EOC and iPP/OBC blends were examined with a Perkin-Elmer differential scanning calorimeter (DSC 7). The instrument was calibrated by indium before measurement. The samples for DSC measurements (about 2–4 mg) were cut from the middle of injection specimens. The samples were heated to 200°C, held for 5 min to remove the thermal history, and then cooled to 40°C. Finally, the samples were heated to 200°C. Both the heating and cooling rate were 10°C/min. All the measurements were under nitrogen atmosphere.

Rheological measurements

A dynamic mechanical spectrometer, TA ARES-G2, was used to obtain the apparent viscosity of the elastomers and iPP from the oscillatory shear measurements at 190°C. The parallel plates with 25 mm diameter were used for all the oscillatory shear measurements. Stress-strain curves were measured

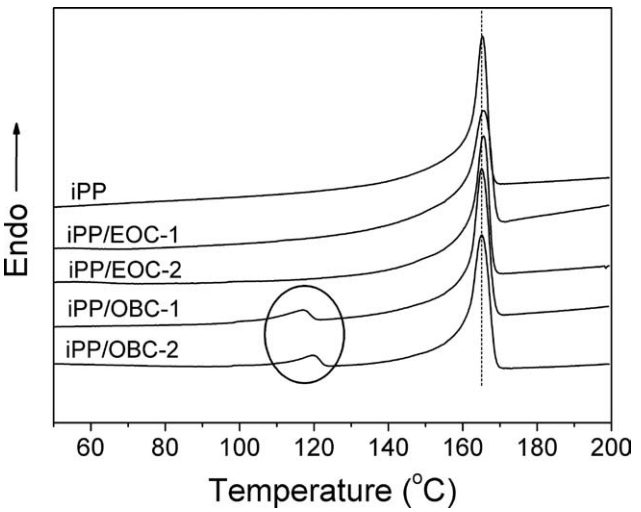

Figure 1 DSC heating curves of iPP and iPP/elastomer blends.

for all the samples to determine the linear viscoelastic region. The strain of the frequency scan for all the samples was 5%.

Scanning electron microscopy (SEM)

A JSM-6700F JEOL SEM (operated at 5 kV) was applied to examine the phase morphology of iPP/EOC and iPP/OBC blends. All SEM specimens were coated with ~ 5 nm thick of gold/palladium to avoid charging and thereby improving image quality.

Undeformed molded specimens were examined by cryo-fracturing to obtain a survey of elastomer domain size and dispersion. For this purpose, the samples were given a sharp notch, immersed in liquid nitrogen for 5 min, and immediately broken by hand. The resulting fractured surface was etched with xylene at room temperature to remove the elastomer phase from the iPP matrix. The SEM images were analyzed using Image-J to obtain the average dispersed phase size and its standard derivation. Additionally, SEM was also used to study the morphology of fracture surface of the Izod impact specimens.

Mechanical tests

The tensile and flexural tests were performed on an Instron 3365 universal mechanical testing machine at ambient temperature (26°C, 55% relative humidity) with a crosshead speed of 50 and 2 mm/min, respectively. The notched specimens were tested on an Izod impact machine CSI-137C at ambient temperature (26°C, 55% relative humidity). The hammer used had a maximum energy of 2.71 J. The reported values of the tensile and flexural results had been averaged over at least five independent measurements. At least 10 measurements were averaged for Izod impact tests.

RESULTS AND DISCUSSION

Thermal analysis

The melting behaviors of the blends were investigated by DSC. As shown in Figure 1, the major exothermic peak located at about 165°C corresponded to the melting of iPP. A small peak at about 120°C could be seen for both iPP/OBC-1 and iPP/OBC-2, which corresponded to the melting of OBC. The crystallinity of the iPP component was calculated from the ratio of the fusion enthalpy per normalized gram of iPP in the blend to that of a theoretically 100% crystalline iPP (taken as 209 J/g).[16] The melting temperatures, crystallinities of iPP component for the blends were similar (Table II), indicating that the elastomer phase had no significant influence on the crystal form and crystal perfection of the iPP matrix. Some literatures showed that the elastomer phase could act as a nucleating agent for iPP crystallization, resulting in a decrease of melting temperature and an increase of crystallization temperature.[17] Some other reports showed EOC phase had almost no influence on the melting behavior of iPP,[18] which was similar to our results.

Morphology of iPP/EOC and iPP/OBC blends

The SEM images of iPP/EOC and iPP/OBC blends are shown in Figure 2. The elastomer domains in the four blends were roughly spherical. It can be seen that iPP/EOC-1 formed larger domain sizes than iPP/EOC-2. Similarly, iPP/OBC-1 formed larger dispersed phase sizes than iPP/OBC-2. To obtain quantitative information, the average domain sizes were calculated by analyzing SEM images with an image analysis software image-J, as shown in Figure 3. The dispersed domain size of iPP/EOC-1 was higher than that of iPP/OBC-1, and the dispersed domain size of iPP/EOC-2 was higher than that of iPP/OBC-2.

TABLE II
Melting Temperature and Crystallinity of iPP Component in Pure iPP and Blends

Sample	iPP	iPP/EOC-1	iPP/EOC-2	iPP/OBC-1	iPP/OBC-2
T_m	165.3	165.5	165.6	165.0	165.2
Crystallinity (%)	49.3	48.4	49.6	49.3	49.2

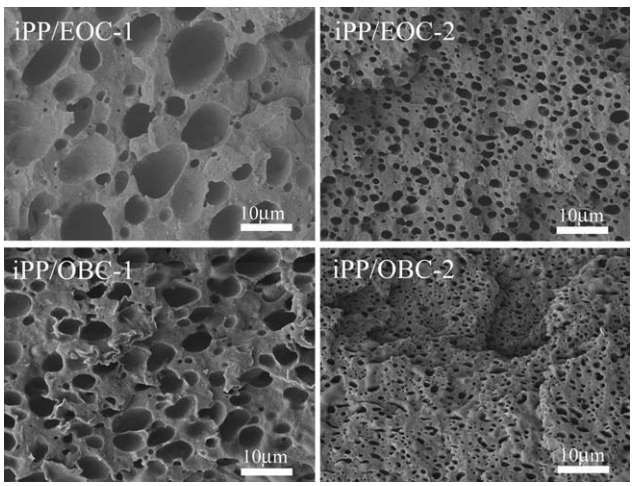

Figure 2 SEM images of iPP/EOC and iPP/OBC blends.

The formation of dispersed phase during melt blending of polymer blends has been studied extensively. There are two factors determining the morphology of immiscible polymer blends: the viscosity ratio η_d/η_m (p) and interfacial tension. The dispersed particle size is proportional to interfacial tension and $p^{0.84}$ when $p > 1$ or $p^{-0.84}$ when $p < 1$.[19] Therefore, binary blends with the lowest interfacial tension and a viscosity ratio close to unity would form the smallest dispersed phase particles. Figure 4 is the log-log plot of complex viscosity (η^*) and the investigated shear rates for EOC, OBC, and pure iPP. In the whole range of explored shear rate, all four elastomers and iPP exhibited a decrease in viscosity with increasing shear rates, indicating pseudoplastic characteristics. It was also observed that the viscosity curve of EOC-1 was close to that of OBC-1, and the viscosity curve of EOC-2 was close to that of OBC-2 in the investigated shear rate range. It can be seen that p is higher than 1 for both iPP/EOC and iPP/OBC blends. However, the viscosity ratios of the blends with higher MFR elastomers were obviously much smaller than those of blends with smaller MFR elastomers. For elastomers with the same chain composition, the viscosity ratio is the dominant factor controlling the dispersed phase size. Therefore, the lower viscosity elastomers, having viscosities closer to the used iPP, formed smaller dispersed domains in the blends than the higher viscosity ones.

For elastomers with similar viscosities, the dominant controlling factor for dispersed phase size in the blends is the interfacial tension. As shown in Figure 3, block copolymers formed smaller dispersed domains than statistical copolymers with the similar MFR. This result indicated that OBC had lower interfacial tension with iPP than EOC did. Consequently, it could be expected the compatibility between OBC and iPP was better than that between EOC and iPP.

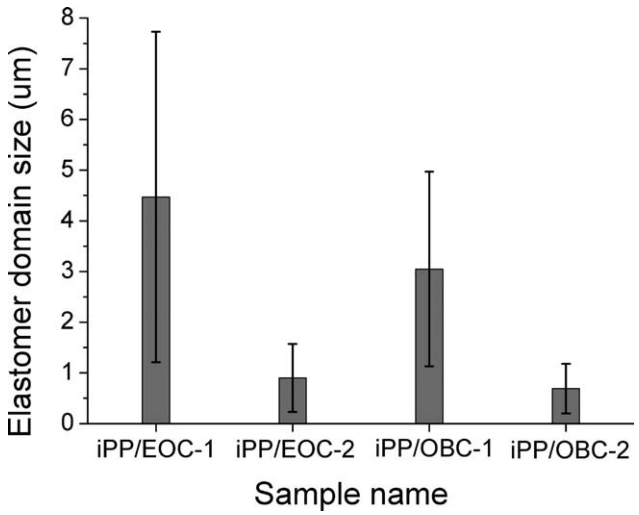

Figure 3 The dispersed phase sizes of iPP/elastomer blends.

Mechanical properties

The engineering stress-strain curves obtained from tensile tests are plotted in Figure 5. As expected, the strain at break increased and the yield stress deceased for blends compared to iPP. Yielding became diffuse with the addition of elastomers. Furthermore, inclusion of elastomers promoted strain hardening phenomenon, and caused higher stress at break, which agreed well with previous reports.[20–23]

Table III summarizes the properties of the blends. Obviously, compared with pure iPP, the blends had higher strain and stress at break, but lower yield stress and modulus. The four blends had similar overall tensile and flexural properties. However, minor differences could be noticed, that is, the performance of iPP/EOC-2 (iPP/OBC-2) was slightly higher than iPP/EOC-1(iPP/OBC-1) in modulus, yield stress, stress and strain at break, indicating

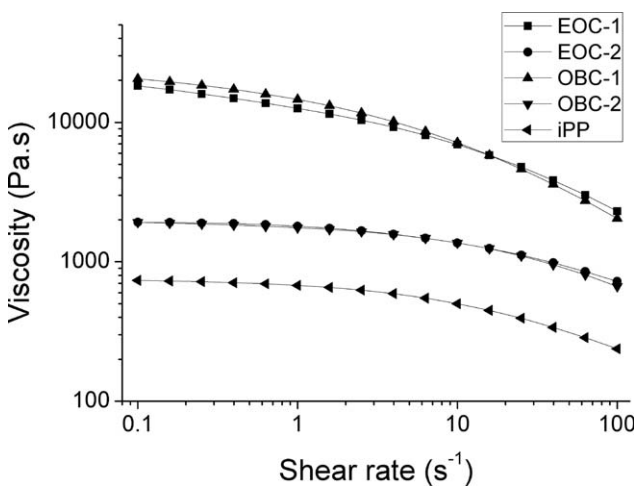

Figure 4 Apparent viscosity versus shear rate for the elastomers and pure iPP at 190°C.

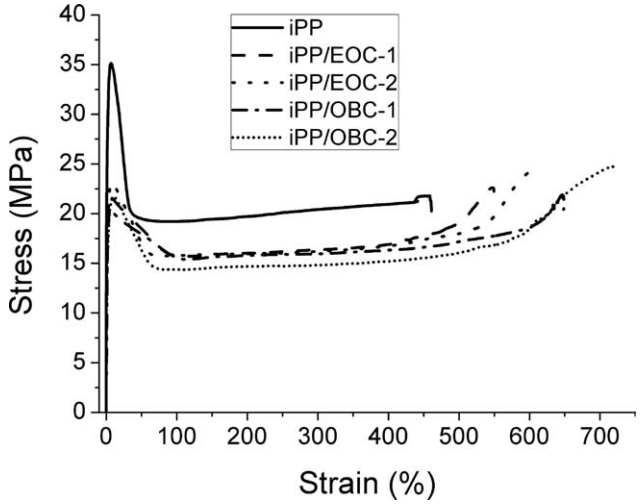

Figure 5 Engineering stress-strain curves of pure iPP and blends.

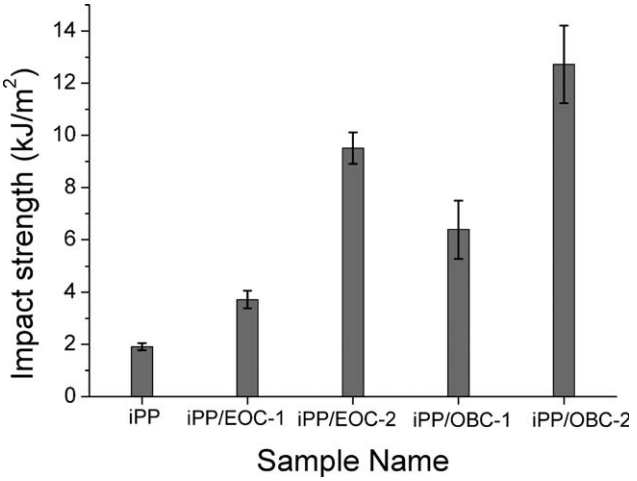

Figure 6 Izod impact strength of iPP/EOC and iPP/OBC blends.

that smaller dispersed size was somewhat beneficial for improving the mechanical properties.

The impact properties of the blends were all greatly enhanced (Fig. 6). The notched Izod impact strength for iPP was only 2 kJ/m^2, which was a typical value for brittle fracture. The toughening effect was not the same for the two kinds of elastomers, with OBC-2 better than EOC-2 (two elastomers had similar MFR), and OBC-1 better than EOC-1(two elastomers had similar MFR). In another comparing way, the impact strength of iPP/OBC-2 was higher than that of iPP/OBC-1, and iPP/EOC-2 higher that iPP/EOC-1. Combining the above morphological analysis in Figure 2, it was concluded that the blend with smaller elastomer domain size attained higher impact strength. The toughness of polymer/rubber blends have been studied since the 1970s, and many theories and models, such as crazing, cavitation and shear yielding were proposed.[24–28] Amorphous polymers such as polystyrene and poly(methyl methacrylate) tend to craze, have a low crack initiation and a low crack propagation energy, and therefore have both a low unnotched and a low notched impact toughness. Matrix crazing is the main mechanism of energy dissipation in such polymer/rubber blends. For semicrystalline polymers, crazing and shear yielding usually function interactively in fracture.[29] For rubber toughened iPP, Jang[2,30] found that smaller dispersed particles were more effective in toughening iPP than larger ones, probably because the former case represented a more efficient use of rubbery phase in promoting crazing and/or shear yielding. The iPP blends exhibited pronounced crazing when the average diameter (D) of rubber particles was larger than or equal to 0.5 μm. No crazes appeared to develop around individual rubber particles with $D < 0.5$ μm, indicating that the behavior was dominated by shear yielding.[30] The elastomer phase in all the blends of this study, were all larger than 0.5 μm, thus being capable of initiating crazes.

Macroscopically, the fracture surfaces of the blends were rougher than that of iPP and some degree of whitening was observed (Fig. 7). The fracture surface of iPP showed no whitening, indicating a typical brittle fracture. For iPP/EOC-1 and iPP/OBC-1 blends, whitening could be observed at the notch, and the whitening zone of iPP/OBC-1 was larger than that of iPP/EOC-1. As to iPP/EOC-2 and iPP/OBC-2 blends, partial break with remarkable whitening could be observed, and the whitening

TABLE III
Tensile and Flexural Properties of iPP/EOC and iPP/OBC Blends

Sample	Flexural modulus[a] (MPa)	Yield stress (MPa)[b]	Stress at break[b] (MPa)	Strain at break[b] (%)
iPP	1423 ± 16	35.4 ± 0.2	21.0 ± 2.6	510 ± 120
iPP/EOC-1	736 ± 9	21.4 ± 0.2	20.7 ± 1.5	560 ± 30
iPP/EOC-2	824 ± 9	23.1 ± 0.1	22.3 ± 3.8	590 ± 50
iPP/OBC-1	769 ± 6	20.4 ± 0.4	22.6 ± 3.3	690 ± 70
iPP/OBC-2	807 ± 25	22.5 ± 0.2	25.9 ± 0.2	720 ± 20

[a] Determined from flexural tests.
[b] Determined from tensile tests.

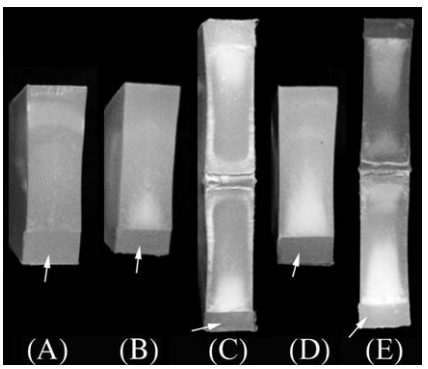

Figure 7 Photograph of fractured surface after Izod impact tests. (A) iPP; (B) iPP/EOC-1; (C) iPP/EOC-2; (D) iPP/OBC-1; (E) iPP/OBC-2. The arrows show the notch position.

zone of iPP/OBC-2 was larger than that of iPP/EOC-2. The SEM micrographs in Figure 8 gave a closer look at these Izod fracture surfaces. For all the four blends, nearly no shear yielding was observed, which could be attributed to the large dispersed particle size as mentioned before. Additionally, there was little deformation of the elastomer particles of iPP/EOC-1 and iPP/OBC-1. Conversely, the elastomer phase experienced obvious deformation after impact tests for iPP/EOC-2 and iPP/OBC-2. From the above results, crazing was probably the main mechanism of energy dissipation for the four blends. Under a constant elastomer fraction, the amount of crazes increased with increasing the number of particles. Smaller elastomer particles were therefore more efficient in toughening iPP than larger ones.

It is difficult to compare iPP/EOC and iPP/OBC blends in a direct manner, because both elastomer particle size and interfacial adhesion have to be considered. Recent studies showed that block olefin copolymers had better adhesion to iPP than statistical copolymers either with the same octene content as the soft segment of block copolymers or with the same overall octene content as the block copolymers.[31,32] Therefore, both stronger adhesion and smaller particle size contributed to higher impact toughness of iPP/OBC blends.

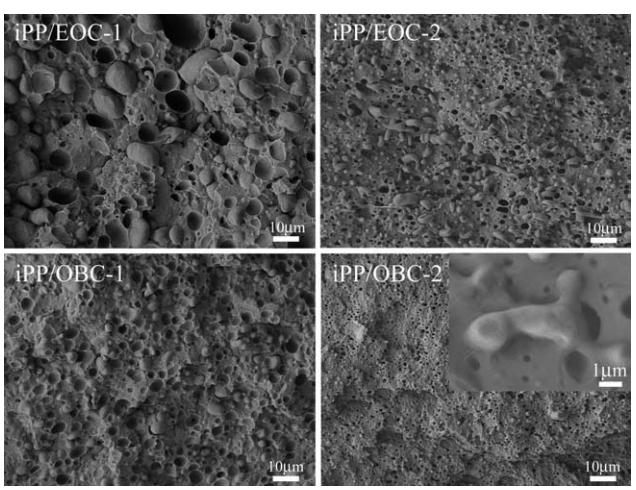

Figure 8 SEM images of fractured surface after Izod impact tests. The inset is the high magnification image.

Based on the analysis of morphology and mechanical properties, it could be concluded that the investigated OBCs were more compatible with iPP than EOCs. As reported previously,[33–35] blends of ethylene-propylene statistical copolymer, ethylene-butene statistical copolymer and ethylene-hexene statistical copolymer with iPP ranged from partially miscible to fully miscible with increasing comonomer content. The type and content of comonomer played a key role in the properties of iPP/statistical copolymer blends and governed the morphology development as well as the thermal behavior and toughness/stiffness balance.[35]

It should be noted that the octene content of the soft segments of the OBCs (>27% mol) was higher than that of EOCs (<14.5% mol), resulting in a greater degree of compatibility between the soft segments of OBC and iPP than statistical copolymers. Additionally, the relatively large amount of soft segments (~ 80% wt) also imparted good compatibility of block copolymers with iPP.

CONCLUSIONS

Blends of iPP with 30 wt % statistical and block ethylene-octene copolymers were prepared by melt blending. The investigated block copolymers formed smaller dispersed particles than statistical copolymers with similar MFRs, and the compatibility between iPP and the investigated block copolymers was better than that between iPP and statistical copolymers.

It is likely that crazing was probably the main mechanism of energy dissipation for the investigated blends. Both strong interfacial adhesion and small dispersed particle size contributed to the high impact toughness of the blends of iPP with block copolymers. The better compatibility between the block copolymers and iPP might be attributed to the higher octene content in the soft segment and sufficiently high soft segment content in block copolymers.

Guoming Liu is debted to Wei Ning (ICCAS) for the rheological measurements.

References

1. Bucknall, C. B.; Page, C. J. J Mater Sci 1982, 17, 808.
2. Jang, B. Z. J Appl Polym Sci 1985, 30, 2485.
3. Yokoyama, Y.; Ricco, T. Polymer 1998, 39, 3675.
4. Liang, J. Z.; Li, R. K. Y. J Appl Polym Sci 2000, 77, 409.
5. Thio, Y. S.; Argon, A. S.; Cohen, R. E.; Weinberg, M. Polymer 2002, 43, 3661.
6. Zuiderduin, W. C. J.; Westzaan, C.; Huetink, J.; Gaymans, R. J. Polymer 2003, 44, 261.

7. Bensason, S.; Minick, J.; Moet, A.; Chum, S.; Hiltner, A.; Baer, E. J Polym Sci Part B: Polym Phys 1996, 34, 1301.
8. Bensason, S.; Nazarenko, S.; Chum, S.; Hiltner, A.; Baer, E. Polymer 1997, 38, 3913.
9. Isasi, J. R.; Haigh, J. A.; Graham, J. T.; Mandelkern, L.; Alamo, R. G. Polymer 2000, 41, 8813.
10. Arriola, D. J.; Carnahan, E. M.; Hustad, P. D.; Kuhlman, R. L.; Wenzel, T. T. Science 2006, 312, 714.
11. Wang, H. P.; Khariwala, D. U.; Cheung, W.; Chum, S. P.; Hiltner, A.; Baer, E. Macromolecules 2007, 40, 2852.
12. Lejiv, M.; Maurer, F. H. J. Polym Eng Sci 1988, 28, 670.
13. Zhou, X. Q.; Hay, J. N. Polymer 1993, 34, 4710.
14. Bains, M.; Balke, S. T.; Reck, D.; Horn, J. Polym Eng Sci 1994, 34, 1260.
15. Flaris, V.; Zipper, M. D.; Simon, G. P.; Hill, A. J. Polym Eng Sci 1995, 35, 28.
16. Alexander L. E. X-ray Diffraction Methods in Polymer Science; Weily-interscience: New York, 1969.
17. Jang, B. Z. J Appl Polym Sci 1985, 30, 2485.
18. McNally, T.; McShane, P.; Nally, G. M.; Murphy, W. R.; Cook, M.; Miller, A. Polymer 2002, 43, 3785.
19. Wu, S. Polym Eng Sci 1987, 27, 335.
20. Bedia, E. L.; Murakami, S.; Senoo, K.; Kohjiya, S. Polymer 2002, 43, 749.
21. Yang, J. H.; Zhang, Y.; Zhang, Y. X. Polymer 2003, 44, 5047.
22. Nitta, K. H.; Shin, Y. W.; Hashiguchi, H.; Tanimoto, S.; Terano, M. Polymer 2005, 46, 965.
23. Pang, Y. Y.; Dong, X.; Zhang, X. Q.; Liu, K. P.; Chen, E. Q.; Han, C. C.; Wang, D. J. Polymer 2008, 49, 2568.
24. Merz, E. H.; Claver, G. C.; Baer, M. J Polym Sci 1956, 22, 325.
25. Schmitt, J. A.; Henno, K. J Appl Polym Sci 1960, 3, 132.
26. Newman, S.; Strella, S. J Appl Polym Sci 1965, 9, 2297.
27. Bucknall, C. B. Toughened Plastics; Applied Science Publisher: London, 1977.
28. Wu, S. H. J J Polym Sci Polym Phys Ed 1983, 21, 699.
29. Galeski, A. Prog Polym Sci 2003, 28, 1643.
30. Jang, B. Z.; Uhlmann, D. R.; Vandersande, J. B. Polym Eng Sci 1985, 25, 643.
31. Dias, P.; Lin, Y. J.; Poon, B.; Chen, H. Y.; Hiltner, A.; Baer, E. Polymer 2008, 49, 2937.
32. Kamdar, A. R.; Ayyer, R. K.; Poon, B. C.; Marchand, G. R.; Hiltner, A.; Baer, E. Polymer 2009, 50, 3319.
33. Yamaguchi, M.; Miyata, H.; Nitta, K. H. J Appl Polym Sci 1996, 62, 87.
34. Nitta, K. H.; Shin, Y. W.; Hashiguchi, H.; Tanimoto, S.; Terano, M. Polymer 2005, 46, 965.
35. Maeder, D.; Thomann, Y.; Suhm, J.; Mulhaupt, R. J Appl Polym Sci 1999, 74, 838.